Formation of liquid phase and nanostructures in flash sintered ZnO

Xin Li Phuah[1], Wolfgang Rheinheimer[1,2], Akriti[3], Letian Dou[3] & Haiyan Wang[1,4*]

[1] School of Materials Engineering, Purdue University, West Lafayette, IN 47907, USA.
[2] Now at Institute of Energy and Climate Research, Materials Synthesis and Processing (IEK-1), Jülich Research Centre, 52428 Jülich, Germany.
[3] Davidson School of Chemical Engineering, Purdue University, West Lafayette, IN 47907, USA.
[4] School of Electrical and Computer Engineering, Purdue University, West Lafayette, IN 47907, USA.
*Corresponding author: hwang00@purdue.edu

Abstract

This study presents the effects of current density limit on flash sintering and the formation of nanostructures in undoped ZnO. The combination of high electric field and low current density (e.g., 1 and 2 A/cm^2) results in the formation of hot spots and fracture as well as ZnO nanostructures in the vicinity of the hot spots. Such phenomena were not observed in the higher current density limit of 3 A/cm^2. A detailed microscopy analysis revealed that the growth of nanostructures initiated from liquid phase regions at the grain boundaries and within the grains.

Keywords: Flash sintering, ZnO, liquid phase, nanostructures, electromigration

Flash sintering was first reported a decade ago and has gained significant attention due to its unique capability of densifying ceramics within a few seconds [1]. This technique is performed by applying an electric field to a green body during the heating process. At a certain combination of furnace temperature and electric field, the sample starts to be conductive enough and begins to flow current. This causes the sample to experience Joule heating and a thermal runaway, which rapidly increases the sample temperature over the furnace temperature. The non-equilibrium characteristics of this phenomenon has resulted in many unique features, such as a generation of high density of defects and metastable phases [2–6].

In a recent study, flash sintering of ZnO performed with high electric field and low current density has shown a unique capability of forming nanostructures [7]. ZnO nanostructure growth commonly occurs by the vapor-liquid-solid mechanism, which requires the presence of a liquid phase as nucleation sites. However, the formation of liquid phase in ZnO has only been observed in systems containing metallic oxide additives, where the additive has a low melting temperature such as Bi_2O_3 ($T_m \sim 875°C$) [8,9]. In this study, microstructural evidence of the formation of liquid phases and nanostructures in flash sintered ZnO is presented under various current density conditions, and correlated with the photoluminescence characteristics. The formation mechanisms are discussed.

Commercial ZnO nanopowder (US Research Nanomaterials Inc, 99.95% purity) with an average particle size of 18 nm was pressed into cylindrical green bodies (diameter of 6 mm, thickness of 3 mm, green density of ~60%). Flash sintering was performed in a horizontal push-rod dilatometer (TA Instruments DIL 801), where the green body was placed between two Pt coils as contact which were connected to a DC power supply (Sorenson DLM 300-2). While the furnace was heating to 900°C at 25°C/min, an electric field of 600 V/cm was applied across the sample.

The power supply automatically switches from voltage to current control when the current density reaches the preset limit during heating. In this study, three samples with a current density limit of 1, 2 and 3 A/cm^2 were compared. The steady state current was held for 60 seconds before turning off the power supply. The furnace was cooled at 25°C/min after reaching the furnace temperature of 900°C. The microstructure of the fractured surface was characterized by a Quanta 650 FEG scanning electron microscope (SEM). Photoluminescence (PL) was performed at room temperature using a Coherent OBIS laser with a wavelength of 375 nm and collected by a SpectraPro HRS-300 spectrometer.
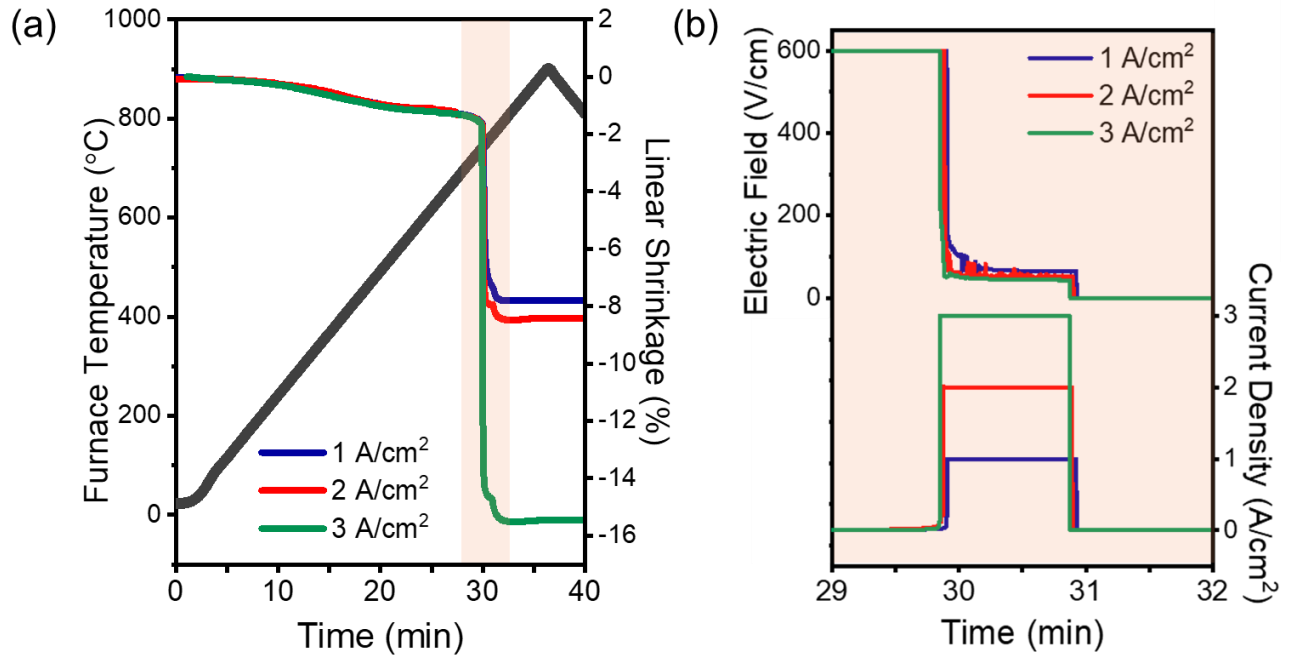

Fig. 1. (a) Furnace temperature and linear shrinkage measured by the dilatometer during flash sintering with current density limits of 1, 2 and 3 A/cm^2. (b) Electric field and current density curves between 29 and 31 minutes, where the power supply switches from voltage to current control.

The furnace temperature and linear shrinkage measured by the dilatometer are shown in Fig. 1a during the entire heating process. At approximately 750°C, both abrupt current flow and shrinkage were observed for all samples. The sample experienced more total shrinkage with higher current densities due to the higher expected sample temperature caused by the higher power dissipation. Fig. 1b shows the electric field and current density curves between 29 and 31 minutes of the heating process. When the power supply is turned off after the holding time, a drop of sample temperature and a slight dip in the linear shrinkage curves is evident in Fig. 1a.
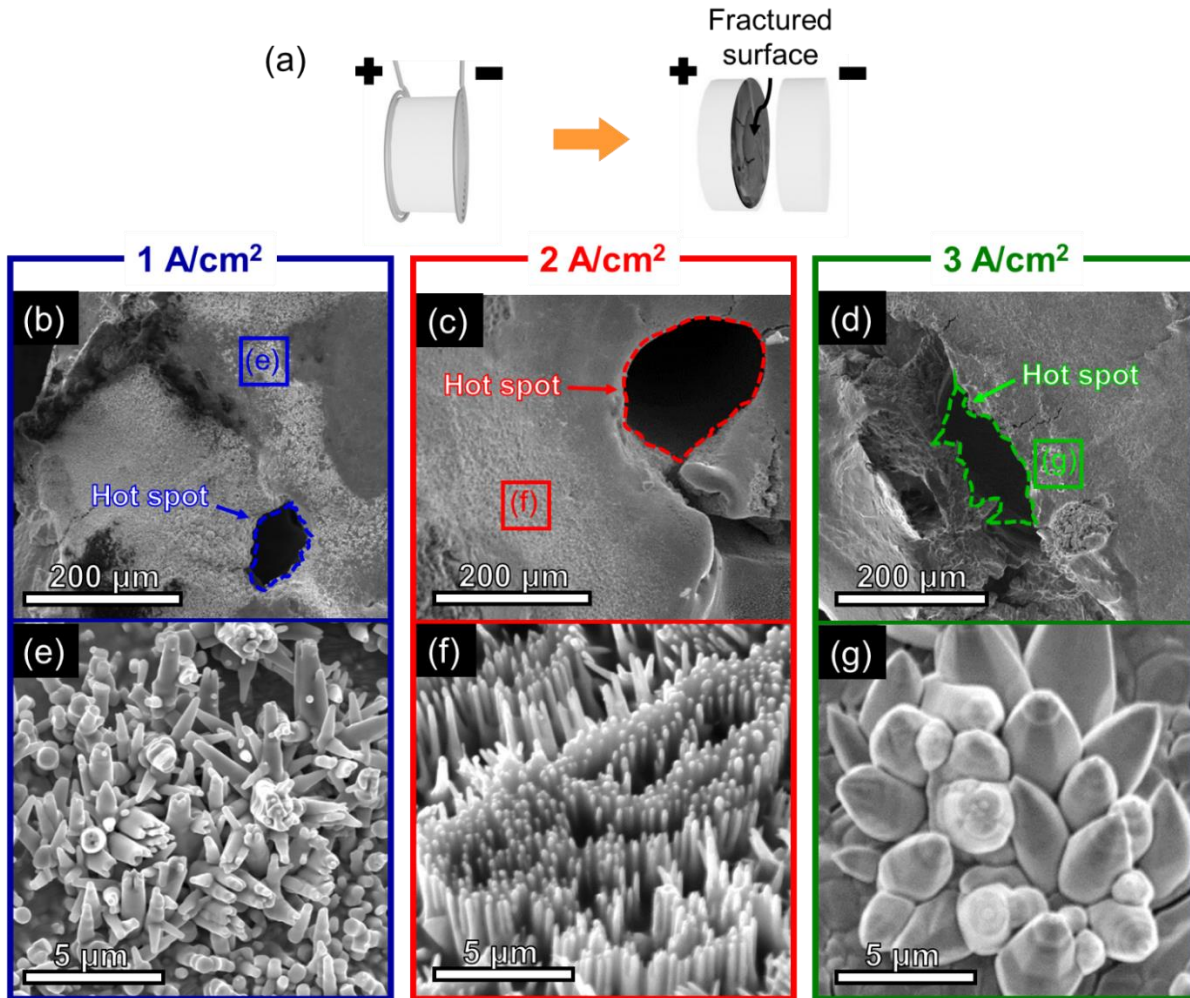

Fig. 2. (a) Schematic of sample fracture Low magnification SEM of samples with current density (b) 1 A/cm2, (c) 2 A/cm^2 and (d) 3 A/cm^2, showing the overall morphology of fractured surface (positive) containing large void. (c) Higher magnification of the area marked by the box in (b) showing the various morphology of nano- and microstructure formed.

In previous flash sintering studies of ZnO, the minimum current density required to reach high relative densities ($> 95\%$) is at least 4 A/cm^2 [4,9,10]. Instead, by using a combination of very high electric field and low current densities, very fast shrinkage occurred, along with fracture approximately midway through the sample and parallel to the electrodes (Figure 2(a)). A previous study showed a large void and the growth of nanostructures in the vicinity of the void on the positive fractured surface [7]. Thus, in this study, only the positive fractured surface was further investigated for each current density.

Fig. 2b-d show low magnification SEM images of the positive fractured surfaces of samples with current density of 1, 2 and 3 A/cm^2, respectively. In each of the images, a large void with a diameter of several hundred microns was observed, which is the result of a hotspot as discussed later. Fig. 2e-g shows the area near the void, where the growth of nano- and microstructures was observed. These structures had different morphology at each current density. For the sample with a current density limit of 1 A/cm^2, the nanostructures resembled tetrapods, while using a current density limit of 2 A/cm^2 formed well-aligned nanorods. On the contrary, current density limit of 3 A/cm^2 results only in the growth of large rods with diameters of 3 to 5 μm containing hexagonal facets and tapered pyramidal ends. This contrasting observation suggests different growth mechanisms occurring between the low (1 and 2 A/cm^2) and high current densities (3 A/cm^2).
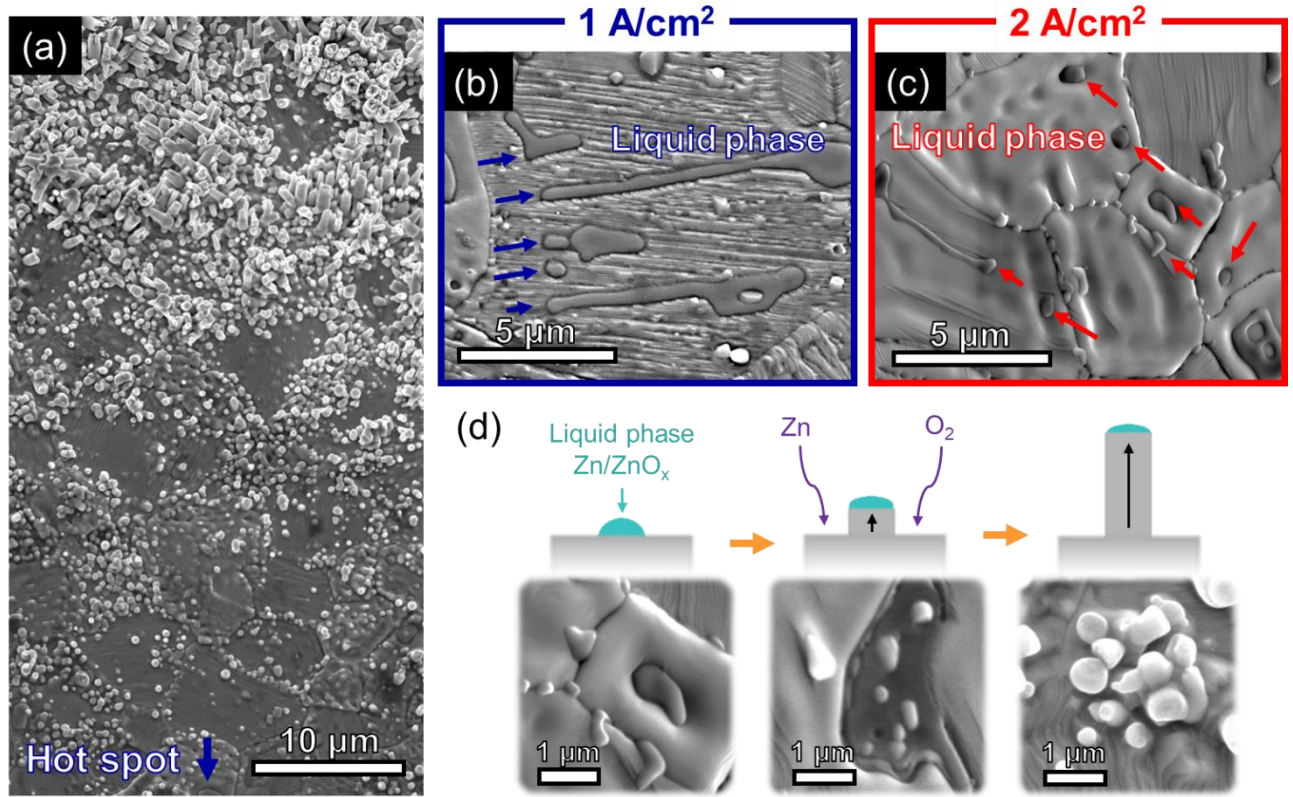
Fig. 3. (a) SEM showing the gradient in microstructure which exist between the nanostructures and the hot spot areas for the 1 A/cm² sample. The grains with less growth of nanostructures showed liquid phase present in the grains and at the grain boundaries for both (b) 1 A/cm² and (c) 2 A/cm² samples. (d) Schematic of the vapor-liquid-solid mechanism.

The low current density samples containing nanostructures were further analyzed to investigate the growth mechanism. Figure 3a shows a gradient of microstructure between the nanostructures region and the hot spot. This image revealed that the nanostructures grew on very large grains (~3 to 10 μm) and mostly around the grain boundaries. In some areas, the nanostructure also grew within the grains but less frequently. Upon closer inspection of the large grains without nanostructures, liquid phase regions were observed, as shown in Figure 3b and c for samples with current density limits of 1 A/cm² and 2 A/cm², respectively.

Growth mechanisms of ZnO nanostructures have been explained by vapor-liquid solid (VLS) or vapor-solid (VS) mechanisms. Although the mechanism is difficult to distinguish and it

is possible for both mechanisms to occur in the present case, the direct microstructural evidence of liquid phase shown in the lower current density samples points towards the VLS mechanism. The VLS mechanism is usually associated with the use of a metal catalyst, where the Zn vapor forms a liquid alloy with metal on the substrate and the supersaturation of the liquid will lead to axial growth by precipitation [11]. This can also occur without the use of a catalyst, but would first require the nucleation of Zn/ZnO_x liquid phase [12,13]. In our study, liquid phases observed in Fig. 3(b) and (c) are likely to act as the self-catalyst sites for the growth of nanostructures in the low current density samples, as sketched in Figure 3d. Due to the differences in local temperature and oxygen partial pressure, the resulting morphology of the structures were varied between the samples.

In contrast, the VS mechanism occurs by direct absorption of gas phase onto the solid surface and is likely experienced by the sample with higher current density. Low magnification SEM of the 3 A/cm^2 sample shown in Fig. S1 did not exhibit any liquid phase and the growth of microstructures occurred very scarcely. VS typically occurs at a much slower rate as the nucleation conditions are less favorable without the liquid phase [14]. Additionally, structures produced by the VS mechanism has shown more inhomogeneity. This can be attributed to local thermal fluctuations at the growth front and mobility differences of atoms absorbed on various planes [15,16].
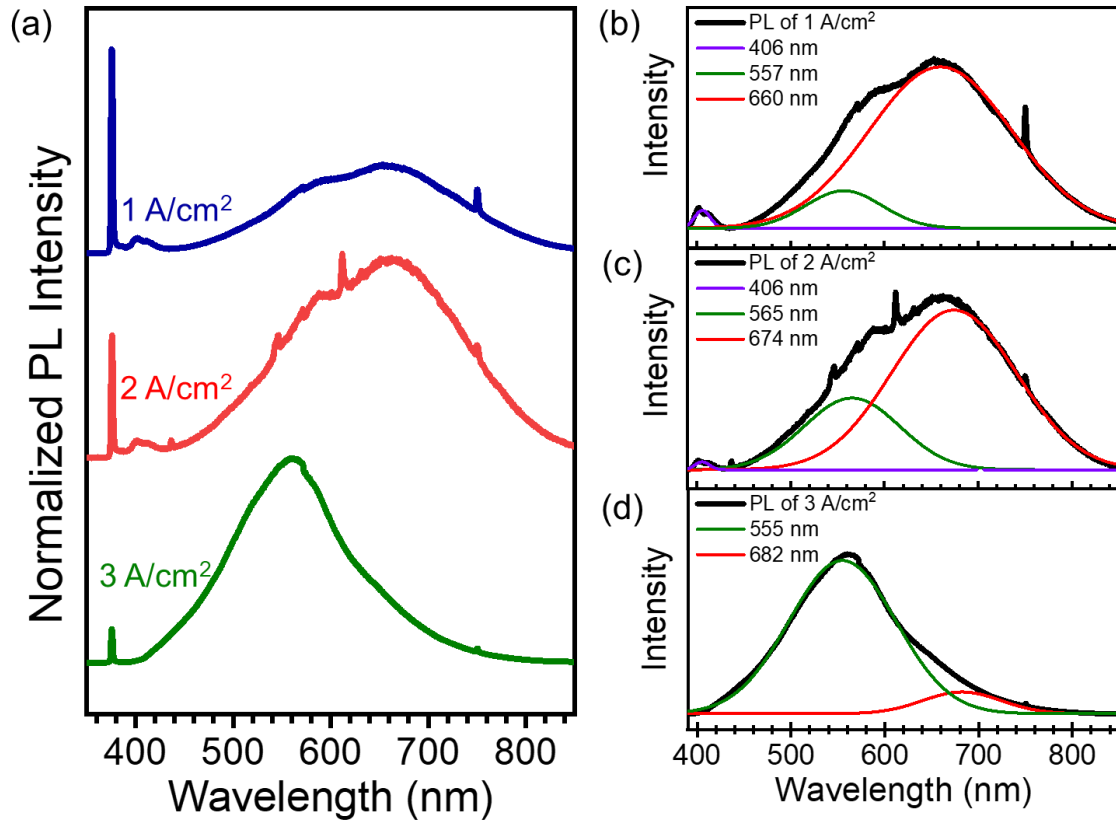
Fig. 4. (a) Room temperature photoluminescence (PL) spectra measured on the positive fractured surface for 1, 2 and 3 A/cm². Deconvolution of the visible emission is shown for (b) 1 A/cm², (c) 2 A/cm² and (d) 3 A/cm².

To understand the occurrence of nanostructures during flash sintering, first the formation of the crack needs to be addressed. As shown in Fig. 2, cracking is associated with the formation of a hot spot. The hot spot is the result of having a preferred current percolation pathway which causes local overheating. This phenomenon is typically observed in large cross-sectional samples and extreme flash conditions such as high electric fields and current densities [8]. The formation of a large void as evident in Fig. 2 would also suggest that thermodynamic conditions resulted in the formation of liquid or gas phase of ZnO, i.e., the ZnO was driven off-stoichiometric and/or the temperature increased to above 2000°C [15]. Due to volume changes arising from phase transformations, the formation of cracks and sample fracture are likely to occur. While the reason

for the cracking remains unclear, it seems clear that it occurred in the beginning of flash sintering, when strong temperature gradients and high temperatures develop as nanostructures could not have formed otherwise. Note that the cracking event is not visible in the densification curves in Fig. 1a.

Within the crack, the thermodynamic conditions were such that nanorods formed [cite the nanotech paper]. As nanostructure sin ZnO are usually associated with point defects, the point defect concentrations where analyzed at the positive fractured surface of all three samples by room temperature photoluminescence (PL) as shown in Fig. 4a. Typical PL spectra for ZnO consist of a UV or near band-edge (NBE) peak and one or several broad emission peaks in the visible range from deep level emissions (DLE) [17]. The peak at 375 nm corresponds to the UV emission, which is based on free exciton emission, while the broad overlapping peaks above 375 nm correspond to visible emissions from point defects. The ratio of UV to visible emission showed a decreasing trend with increasing current densities, as a higher current density results in a higher point defect concentration.

To investigate the origin of DLE peaks, deconvolution of the visible region was performed for all three samples in Fig. 4b-d using Gaussian fitting. Three peaks are identified at about 406 nm, 560 nm and 670 nm corresponding to V'_{Zn}, $V^{°}_{O}$ and O'_{i}, respectively [18,19]. While the position of these three peaks changes slightly with varying current limits, the relative intensities change strongly. The peak at 410 nm (V'_{Zn}) disappears completely at 3 A/cm². The peak at 650nm (O'_{i}) decreases as well with increasing current limit, but the peak at 550 nm ($V^{°}_{O}$) increases significantly. Accordingly, the PL spectra indicate the following effects with increasing current limit: an overall increasing surface defect concentration, a relative decrease of $[V'_{Zn}]$ and $[O'_{i}]$ and a relative increase of $[V^{°}_{O}]$. These changes agree well with a reduction of the surface [18] and with the occurrence of

a liquid phase as observed in Fig. 3 that only exists between 692K and 1179K in reducing conditions [20].

Based on these defect characteristics, it is likely that a surface reduction of the positive crack surface occurred during flash sintering either by electromigration or by nucleation of point defects. Electromigration [21–23] and a reduction [cite] are well-known for flash sintering and seems the most likely source. The electric field in the sample could migrate oxygen vacancies away from the positive electrode (i.e. towards the positive side of the crack). Zn vacancies could migrate towards the negative electrode (i.e. away from the positive side of the crack).

In summary, flash sintering of ZnO under various current densities were investigated. All samples experienced a hot spot with a large void and fracture which occurred parallel to the electrodes as a result from the volume changes from phase transformations to gas and/or liquid phase(s). Samples with current densities 1 and 2 A/cm^2 resulted in a field assisted growth of nanostructures in the vicinity of the hot spot. The growth occurred by the VLS mechanism due to the observation of liquid phases forming within the grains and at the grain boundaries. Increasing the current density to 3 A/cm^2 results in no liquid phase formation. Instead the inhomogeneous microstructures were formed by the VS mechanism. The PL emission indicates an overall increase of point defects with increasing current density, a relative decrease of $[V'_{Zn}]$ and $[O'_i]$ and a relative increase of $[V^{\circ}_O]$ indicating a reduction of the positive side of the crack during flash sintering. This reduction is likely to be caused by electromigration. This work documents the impacts of electric fields and currents during flash sintering on the stoichiometry of ZnO. The results offer new pathways to design non-stoichiometric materials with new functionalities, and field-assisted growth of nanostructures in ZnO.

Acknowledgements

References

[1]   M. Cologna, B. Rashkova, R. Raj, J. Am. Ceram. Soc. 93 (2010) 3556–3559.

[2]   H. Wang, X.L. Phuah, J. Li, T.B. Holland, K.S.N. Vikrant, Q. Li, C.S. Hellberg, N. Bernstein, R.E. Garcia, A.K. Mukherjee, X. Zhang, H. Wang, Ceram. Int. 45 (2018) 1251–1257.

[3]   H. Wang, X.L. Phuah, H. Charalambous, S.K. Jha, J. Li, T. Tsakalakos, X. Zhang, H. Wang, Materialia 8 (2019).

[4]   X.L. Phuah, H. Wang, H. Charalambous, S.K. Jha, T. Tsakalakos, X. Zhang, H. Wang, Scr. Mater. 162 (2019) 251–255.

[5]   H. Charalambous, S.K. Jha, J.S. Okasinski, T. Tsakalakos, Scr. Mater. 190 (2021) 22–26.

[6]   J.M. Lebrun, T.G. Morrissey, J.S.C. Francis, K.C. Seymour, W.M. Kriven, R. Raj, J. Am. Ceram. Soc. 98 (2015) 1493–1497.

[7]   X.L. Phuah, J. Cho, Akriti, L. Dou, W. Rheinheimer, R.E. Garcia, X. Zhang, H. Wang, Nanotechnology (2020) in press.

[8]   D. Dey, R.C. Bradt, J. Am. Ceram. Soc. 75 (1992) 2529–2534.

[9]   Y. Zhang, J.-I. Jung, J. Luo, Acta Mater. 94 (2015) 87–100.

[10]   Y. Zhang, J. Nie, J.M. Chan, J. Luo, Acta Mater. 125 (2017) 465–475.

[11]   Y. Wu, P. Yang, J. Am. Chem. Soc. 123 (2001) 3165–3166.

[12]   M. Wei, D. Zhi, J.L. MacManus-Driscoll, Nanotechnology 16 (2005) 1364–1368.

[13]   B.D. Yao, Y.F. Chan, N. Wang, Appl. Phys. Lett. 81 (2002) 757–759.

[14]   D.A. Grynko, A.N. Fedoryak, O.P. Dimitriev, A. Lin, R.B. Laghumavarapu, D.L. Huffaker, Surf. Coatings Technol. 230 (2013) 234–238.

[15]   R.L. Schwoebel, J. Appl. Phys. 38 (1967) 1759–1765.

[16]   S. Ambrosini, M. Fanetti, V. Grillo, A. Franciosi, S. Rubini, AIP Adv. 1 (2011).

[17]   K. Vanheusden, W.L. Warren, C.H. Seager, D.R. Tallant, J.A. Voigt, B.E. Gnade, J. Appl. Phys. 79 (1996) 7983–7990.

[18]   X.L. Wu, G.G. Siu, C.L. Fu, H.C. Ong, Appl. Phys. Lett. 78 (2001) 2285–2287.

[19]   Y. Li, G.W. Meng, L.D. Zhang, F. Phillipp, Appl. Phys. Lett. 76 (2000) 2011–2013.

[20]   J. Li, L.L. Kerr, Opt. Mater. (Amst). 35 (2013) 1213–1217.

[21]   W. Rheinheimer, J.P. Parras, J.-H. Preusker, R.A. De Souza, M.J. Hoffmann, J. Am. Ceram. Soc. 102 (2019) 3779–3790.

[22]   W. Rheinheimer, X.L. Phuah, H. Wang, F. Lemke, M.J. Hoffmann, H. Wang, Acta Mater. 165 (2019) 398–408.

[23]   W. Rheinheimer, M. Fülling, M.J. Hoffmann, J. Eur. Ceram. Soc. 36 (2016) 2773–2780.